

## Modeling Particulate Bed Electrode for Metal Recovery

*R.Thilakavathi<sup>1</sup>, N.Balasubramanian<sup>2,\*</sup>, C. Srinivasakannan<sup>3</sup>, Ahmed Al Shoaibi<sup>3</sup>*

<sup>1</sup>SRM University, Kattankulathur, Chennai

<sup>2</sup>A.C.Tech, Anna University-Chennai

<sup>3</sup>The Petroleum Institute, Abu Dhabi

\*E-mail: [nbsbala@annauniv.edu](mailto:nbsbala@annauniv.edu)

*Received:* 18 November 2011 / *Accepted:* 24 December 2011 / *Published:* 1 February 2012

---

A theoretical model has been developed to predict bed thickness and hydrodynamic behavior of conducting particles in an expanded bed used for heavy metal removal. Two-dimensional model has been developed to predict the particle behavior in expanded bed electrode. Model equations have been developed for electrode thickness and bed porosity. The effect of particle size on metal recovery has been critically examined. The present model simulations have been compared with the experimental data reported in literature.

---

**Keywords:** Expanded bed electrode, metal removal, bed expansion, electrode thickness, Potential distributions

### 1. INTRODUCTION

The exponential industrial growth and day-to-day changes in human life style have resulted in increased volume and complexity of effluent to the environment. Heavy metal contamination in industrial effluent becomes a serious issue due to its detrimental effect on human health and environment. The heavy metals include cadmium, chromium, cobalt, copper, iron, manganese, mercury, molybdenum, nickel, silver, and zinc. An effluent that contains metal concentrations higher than the acceptable limit, which poses a serious environmental issue due to its detrimental effect on human health. Even an effluent with even low concentrations of heavy metal is extremely toxic, causes several types of pollutions, such as mud formation, exterminate aquatic life and hazards to human health. Hence, the treatment of heavy metal containing industrial effluent becomes indispensable.

Conventionally heavy metals present in the industrial effluents are treated with chemical precipitation, coagulation, adsorption etc. Intrinsic disadvantages of these approaches are higher costs, large space requirements, multi-step processing, and the generation of large amount of solid sludge. Electrochemical techniques have been tried as an alternative to conventional methods for heavy metal removal. In particular, electro deposition of metal present in the industrial effluent is quite attractive in terms of environmental and process economy concern. Using an electrochemical technique, the main reagent is the electron, which is called 'Clean Reagent', and removes the heavy metal present in the effluent without generating any secondary pollutant or bi-product/sludge. The electrochemical technique may offer high removal efficiencies and lower temperature requirements compared to non-electrochemical treatments. Further, the electrochemical method offers advantages such as reintegration of metals into the main process, elimination solid sludge generation etc. Fluidized bed electrodes find increasing applications in many electrochemical processes as they provide enhanced surface area and improved mass transport. The fluidized bed electrode gives high productivity even at low current densities due to its high specific surface area. Further, since the particles are under motion in a fluidized bed electrode, there is little possibility of particle agglomeration due to metal ion deposition. Fluidized bed electrode can be used for continuous operation by removing the grown particles from the reactor without disturbing the deposition process. The electrochemical behavior of fluidized bed particles is significantly influenced by bed expansion, bed height, current density, and the metal concentration.

Extensive work has been reported on fluidized bed electrode for environmental applications. The performance of fluidized bed electrode is very much dependent on the degree of fluidization [1]. Welmers et al. [2] reported the charge transfer mechanism in a fluidized bed electrode. LeRoy [3] proposed a model for electro winning of copper in a fluidized bed electrode using semi continuous operating conditions. Bertrand [4] developed the growth of tin oxide thin films on large hollow Ni particles using the Fluidized Bed Metal–Organic Chemical Vapor Deposition process. Hadzismajlovic et al., [5] demonstrated the electrochemical behavior of metal particles in a fluidized bed electrode in which the bipolar nature was visualised. Couret [6] critically reviewed the application of a fluidized bed electrode for recovery of metal from dilute solutions. Fluidized bed electrode has also been tried for organic pollutant degradation [7]. In our earlier work [8, 9] a fluidized bed electrode has been modeled based on core-annulus and layer growth concepts. Though a good amount of some literature has been reported on fluidized bed electrodes, the influence of hydrodynamic parameters on fluidized bed electrode is considered lacking. In the present work, two-dimensional model has been developed to predict the particle behavior in expanded bed electrode. The influence of bed porosity on limiting current density and mass transfer coefficient is critically examined.

## 2. MODEL DEVELOPMENT

In an expanded bed electrode, when the electrolyte velocity exceeds the minimum fluidization velocity, the particulate bed expands smoothly and the particles rise to the upper layer and fall down.

This will enhance mixing of the dispersed phase. A further increase in the electrolyte velocity will cause the bed to expand vigorously resulting in improved solids mixing. The particle behavior in expanded bed is incorporated into the general theoretical framework of the porous electrode. The conductive particles act as electrodes which are fluidized by the electrolyte flow [Figure 1].

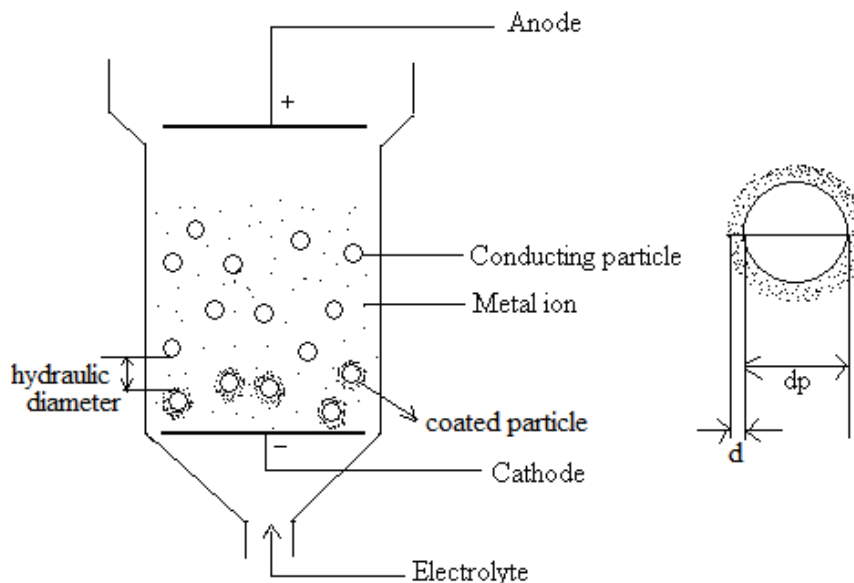


**Figure 1.** Schematic diagram of fluidized bed electro winning process.

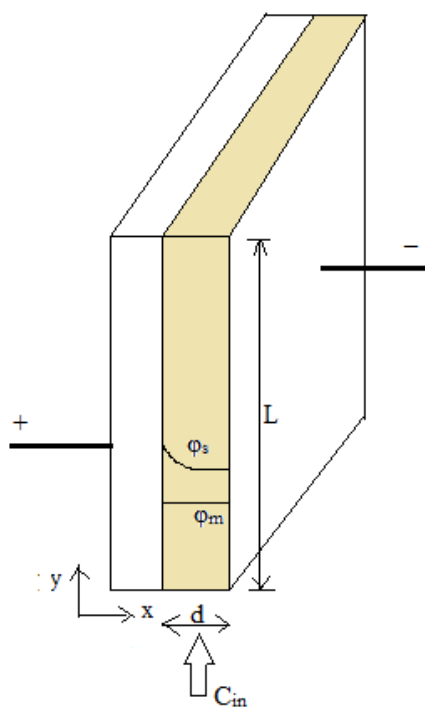


**Figure 2.** Schematic diagram of a two-dimensional model.

The electrode reactions proceed on the electrode surfaces due to an applied charge. Several models have been proposed to describe the flow behavior of solids particles in the expanded bed. In the present study, the two-dimensional model of the expanded bed electrode is formulated with reference to figure 2. Electrolyte flows in the y-direction with a velocity  $U_1$  through a bed of length L. Current flows perpendicular to the electrolyte in the x-direction from an anode separated from the bed to the cathode feeder at position  $x=d$ . A single electrochemical reduction is assumed to occur throughout the bed at its limiting current density. The following assumptions are considered while developing the model equations.

1. The solution contains an excess of supporting electrolyte and that the conductivity is constant and unaffected by changes in composition.
2. The electrical double layers of particles are charged while contacted with current feeders or other particles which carry different charges, and are then moved to other positions for being discharged by either sharing with other particles or by electrochemical reactions.
3. The particles in the expanded bed contact with other particles and the charges pass through them through electronic conduction. The particle-particle contact exists for a short period of time, disconnected and forms another contact resulting in potential fluctuation in the reactor.
4. The electrode particles have a wide size distribution, uniform density and are distributed uniformly throughout the bed.
5. The metal ions are distributed uniformly throughout the reactor and the metal ions are deposited concentrically around the core of expanded bed particle.
6. The superficial velocity of electrolyte is much higher than the terminal velocity of the single particle

The current consumption in an expanded bed electrode can be estimated by the following equation,

$$I = nF(C_{in} - C_{out})U_1 \quad (1)$$

where  $n$  is the number of electrons involved in the electrochemical reaction (for copper,  $n = 2$ ),  $F$  is the Faraday constant (96485 Coulomb),  $C$  is the metal concentration,  $I$  is the electric current (A) and ' $U_1$ ' represent the electrolyte velocity. For mass transfer controlled reaction the variation of metal concentration along the y-direction can be given as [10],

$$C_{out} = C_{in} \exp\left(\frac{-k_m A_s y}{U_1}\right) \quad (2)$$

The charge balance in the solution is given as,

$$\kappa_s \left( \frac{\partial^2 \phi_m}{\partial x^2} + \frac{\partial^2 \phi_s}{\partial y^2} \right) - nFR(C_{in}, \eta) = 0 \tag{3}$$

Where  $C_{in}$  and  $\eta$  are functions of the dimensions  $x$  and  $y$ . The change in concentration in the  $y$ -direction cause variations in potential in that direction, while the potential in the  $x$ -direction will vary due to the resistivity of the electrolyte. For an electrode material of high conductivity ( $\phi_m$  is constant) the electrolyte potential is obtained by combining equations (2) and (3)

$$\left( \frac{\partial^2 \phi_s}{\partial x^2} + \frac{\partial^2 \phi_s}{\partial y^2} \right) = \frac{A_s n F k_m}{\kappa_s} C_{out} \exp\left(-\frac{A_s k_m y}{U_l}\right) \tag{4}$$

Boundary conditions for the electrode is given as,

$$\begin{aligned} i) \quad x = 0 & \quad \phi_s = 0 \\ x = L & \quad \frac{\partial \phi_s}{\partial x} = 0 \end{aligned}$$

ii) at position  $y=0$  and  $y=L$  no current flows in the  $y$ -direction, i.e.

The solution of equation (4) is solved analytically using the finite Fourier transformation and is given by,

$$\phi(x, y) = \frac{\alpha}{\gamma} (1 - \exp(-\gamma L)) \frac{x(x - 2d)}{2} + 2\alpha\gamma \sum_{n=1}^{\infty} \left| \frac{1 - (-1)^n \exp(-\gamma L)}{(\lambda_n^2 + \gamma^2) \lambda_n^2} \right| \left| \frac{\cosh(\lambda_n (d - x))}{\cosh(\lambda_n d)} - 1 \right| \cos(\lambda_n y) \tag{5}$$

$$\text{Where } \alpha = \frac{A_s n F k_m C_{out}}{\kappa_s L}, \quad \gamma = \frac{A_s k_m}{U_l}, \quad \lambda_n = \frac{n\pi}{L} \tag{6}$$

This infinite series gives the distribution of electrolyte solution potential and electrode potential in the electrode. The potential distribution of equation (5) is approximated with limit of  $\phi_s$  at  $L \rightarrow 0$  and is given as

$$\phi(x, y = 0) = \frac{\alpha d^2}{2} \left( \left(\frac{x}{d}\right)^2 - 2\left(\frac{x}{d}\right) \right) \tag{7}$$

The potential difference across the electrode thickness is given as,

$$\phi_s(d, 0) - \phi_s(0, 0) = \frac{\alpha d^2}{2} = \Delta\phi_s \Big|_{y=0} \tag{8}$$

The electrode thickness is obtained by rearranging equation (14), which is given as,

$$d = \sqrt{\frac{2\kappa_s \Delta\phi_s}{A_s n F k_m C_{out}}} \quad (9)$$

The mean diameter of the coated particles is given as, [9]

$$d_a = d_p + 2d \quad (10)$$

Where  $d$  is the electrode thickness,  $d_p$  is the particle diameter.

The specific surface area of electrode is given by,

$$A_s = \frac{6(1-\varepsilon)}{d_p} \quad (11)$$

The unidirectional potential distribution in electrically conductive electrodes under mass transport controlled conditions can be modeled by neglecting conductivity changes of the electrolyte during electrolysis due to an excess of supporting electrolyte. Therefore electrolyte potential distribution is given as, [13],

$$\phi_s(x) - \phi_s(x=0) = \Delta\phi_s = -\frac{nFU_l C_{in}}{\alpha\kappa_s} [\alpha x + \exp^{-\alpha x} - 1] \quad (12)$$

where  $\phi_s(x)$  is electrolyte potential at  $x$  position within the interstitial spaces of electrode,  $\phi_s(x=0)$  refers the potential at the electrode inlet,  $n$  refers the number of electrons transferred,  $\kappa_s$  refers the conductivity of the electrolyte in the interstitial space of the electrode and  $\alpha$  is the group parameter.

For electrolyte phase

$$\kappa_s = \kappa_{s0} \frac{2\varepsilon}{3-\varepsilon} \quad (13)$$

$$\alpha = \frac{k_m A_s (1-\varepsilon)}{U_l} \quad (14)$$

where  $\kappa_{s0}$  is the pure conductivity of the electrolyte.

Combining equations (1) & (2), we can determine the limiting current produced by the electrode as a function of inlet concentration, specific surface area of electrode  $A_s$  and by assuming uniform concentration the limiting current is given as,

$$I_L = nFU_l C_{in} \left\{ 1 - \exp \left[ \frac{-k_m A_s}{U_l} \right] \right\} \tag{15}$$

Where  $k_m$  is the mass transfer coefficient which is given as, [11]

$$k_m = 0.71U_l \left( \frac{\mu_l}{\rho_l D_s} \right)^{-0.67} \left( \frac{\rho_l U_l d_p}{\mu_l (1-\varepsilon)} \right)^{-0.33} \tag{16}$$

The mass transfer coefficient (eqn. 16) is combined with equation (15) to give overall limiting current, i.e.,

$$I_L = nFU_l C_{in} \left\{ 1 - \exp \left( \frac{0.71U_l A_s}{U_l} \left( \frac{\mu_l}{\rho_l D_s} \right)^{-0.67} \left( \frac{\rho_l U_l d_p}{\mu_l} \right)^{-0.33} \right) \right\} \tag{17}$$

The overall limiting current density is given as,

$$i_L = \frac{I_L}{A_s} = \frac{nFU_l C_{in} \left\{ 1 - \exp \left( \frac{0.71U_l A_s}{U_l} \left( \frac{\mu_l}{\rho_l D_s} \right)^{-0.67} \left( \frac{\rho_l U_l d_p}{\mu_l} \right)^{-0.33} \right) \right\}}{A_s} \tag{18}$$

It can be seen from the above equation that the overall limiting current density is the function of bed porosity, Schmidt number and Reynolds number. Hence the equation (18) can be simplified as

$$i_L = f(\varepsilon, Sc, Re) \tag{19}$$

From equation (19) it can be ascertained that the limiting current density depends on the bed porosity, electrolyte velocity and the particle diameter, i.e.,[12]

$$i_L = 1.24FC_{in} (1-\varepsilon)^{0.57} \varepsilon^{-1.0} U_l^{0.43} d_p^{-0.57} \nu^{-0.1} D^{0.67} \tag{20}$$

The bed porosity during the winning process is given by,

$$\frac{\varepsilon^3}{1-\varepsilon} = \frac{150U_l \mu_l}{g(\rho_s - \rho_l) d_p^2} \tag{21}$$

The bed expansion in liquid-solid expanded bed plays an important role as it directly influences the contact between the phases. The bed expansion of liquid-solid expanded bed can be written as [14]

$$\frac{U_l}{U_t} = \varepsilon^n \tag{22}$$

Where  $U_l$  and  $U_t$  represent the electrolyte velocity and particle terminal velocity. The exponent ‘n’ in equation (22) is function of particle Reynolds number, i.e.,

$$\begin{aligned} n &= 4.65 & \text{Re}_t < 0.4 \\ n &= 4.45 \text{Re}_t^{-0.03} & 0.2 < \text{Re}_t < 1 \\ n &= 4.45 \text{Re}_t^{-0.1} & 1 < \text{Re}_t < 500 \\ n &= 2.39 & 500 < \text{Re}_t \end{aligned} \tag{23}$$

The particle minimum fluidization velocity and terminal velocities are estimated using the following equations. The particle minimum fluidization velocity is given as [9, 15]

$$\frac{\rho_l d_p U_{mf}}{\mu_l} = \left[ (33.7)^2 + 0.0408 \frac{d_p^3 \rho_l (\rho_s - \rho_l) g}{\mu_l^2} \right]^{\frac{1}{2}} - 33.7 \tag{24}$$

The particle terminal velocity can be written as [9]

$$U_t = \frac{g(\rho_s - \rho_l) d_p^2}{18\mu_l} \quad \text{Re} < 0.4 \tag{25}$$

$$U_t = \left[ \frac{4}{225} \frac{(\rho_s - \rho_l)^2 g^2}{\rho_l \mu_l} \right]^{1/3} d_p \quad 0.4 < \text{Re} < 500 \tag{26}$$

$$U_t = \left[ \frac{3.1(\rho_s - \rho_l) g d_p}{\rho_l} \right]^{1/2} \quad 500 < \text{Re} \tag{27}$$

The mean hydraulic diameter as a function of bed porosity is defined in terms of the effective cross sectional area of flow, i.e, the volume of voids  $V_v$ , and the surface area of the solid spherical particles; [16]

$$d_h = \frac{KV_v}{A_s} \quad (28)$$

Where K is constant. Volume of voids is given by  $\frac{V_s \varepsilon}{(1 - \varepsilon)}$ . Where  $V_s$  is the total volume of solids and the surface/volume ratio of the solid spherical particles is given as  $6/d_p$ , and hence the equation (28) can be written as

$$d_h = \frac{Kd_p}{6} \left( \frac{\varepsilon}{1 - \varepsilon} \right) \quad (29)$$

### 3. RESULTS AND DISCUSSION

Table 1 shows the parameters in the simulation and simulated results are given in Figures 3-9. The distribution of potential in electrode is such that at a fixed position  $y$ , the least cathodic point of the electrode is at the current feeder and at a fixed position  $x$ , the least cathodic point is at the cell exit. The variation of electrode thickness across potential drop in an expanded bed electrode is shown in figure 3.

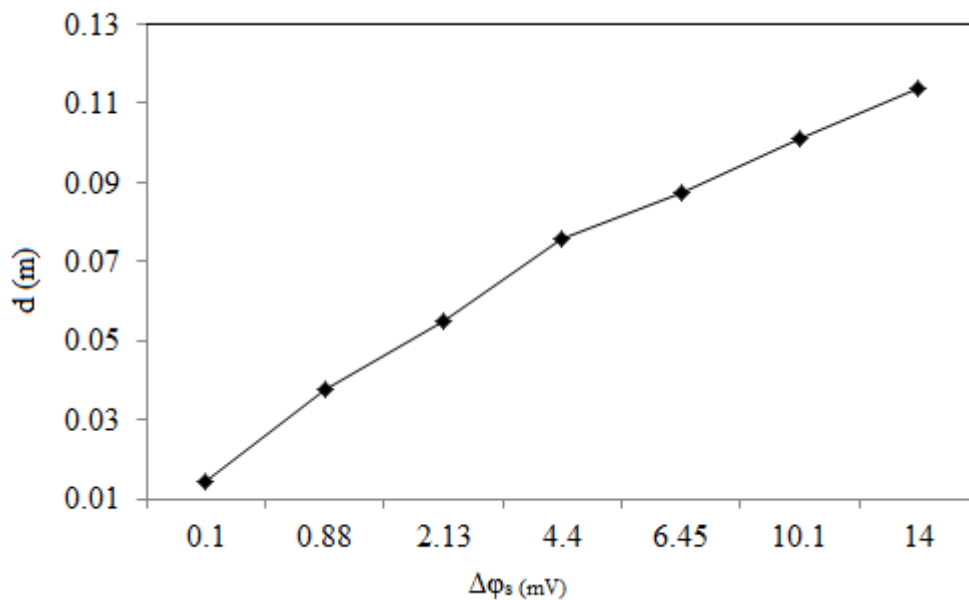


**Figure 3.** The variation electrode thickness across bed potential drop.

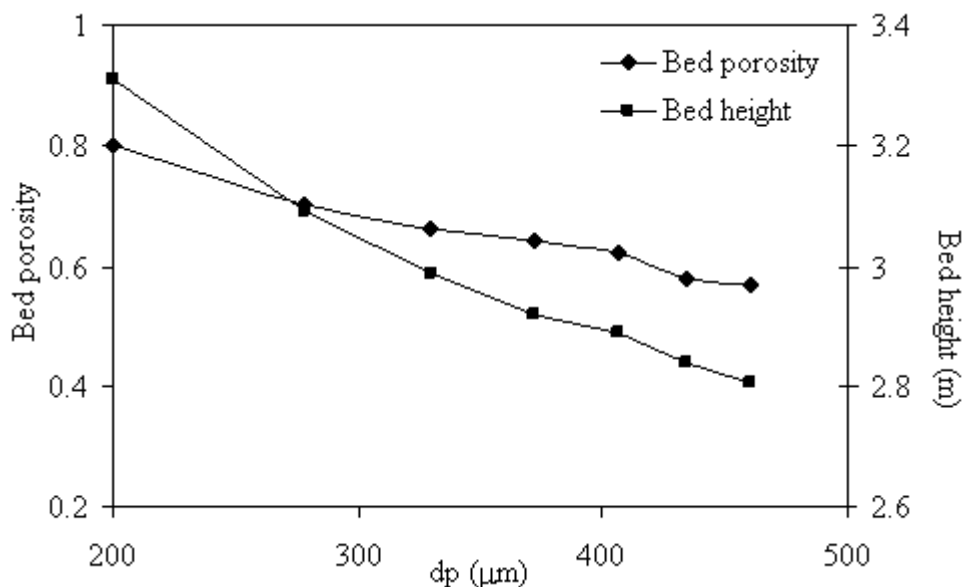


**Figure 4.** The variation bed porosity and bed expansion with particle size.

It can be ascertained from the Figure 3 that electrode thickness increases with increase in potential drop across expanded bed. The dimension which is more significant in determining potential distribution is that in the direction of current flow. The gradual deposit of metal ions on conductive particle would rapidly decrease specific surface area of electrode which in turn increases the electrode thickness (equation 9). With a high electrolyte velocity there is much wider variations in potential drop due to larger current densities applied in bed.

It can be ascertained from the Figure 4 that both bed porosity and bed height decrease with increasing solid particle size. It is a known fact that an increase in the particle size increases the solids hold up resulting in reduction in the bed porosity (equation 21). This can be explained that the effective bed density increases with particle size for a given bed pressure which in turn reduces the bed height, i.e.,

$$\frac{\Delta P}{L} = g(\rho_s - \rho_l)(1 - \epsilon) \tag{30}$$

These observations are in qualitative agreement with our earlier observations [8, 9]. Figure 5 shows the effect of particle size on hydraulic diameter.

It can be noticed that the particle hydraulic diameter decreases with particle size. Though, the hydraulic diameter is directly proportional to the particle size, the cumulative effect of right hand side of the equation (29) decreases with particle size, resulting in reduction in hydraulic diameter with particle size.

The influence of bed porosity and bed expansion on limiting current density has been simulated and the results are given in Figure 6. It can be ascertained that the limiting current density decreases with an increase in the bed porosity.

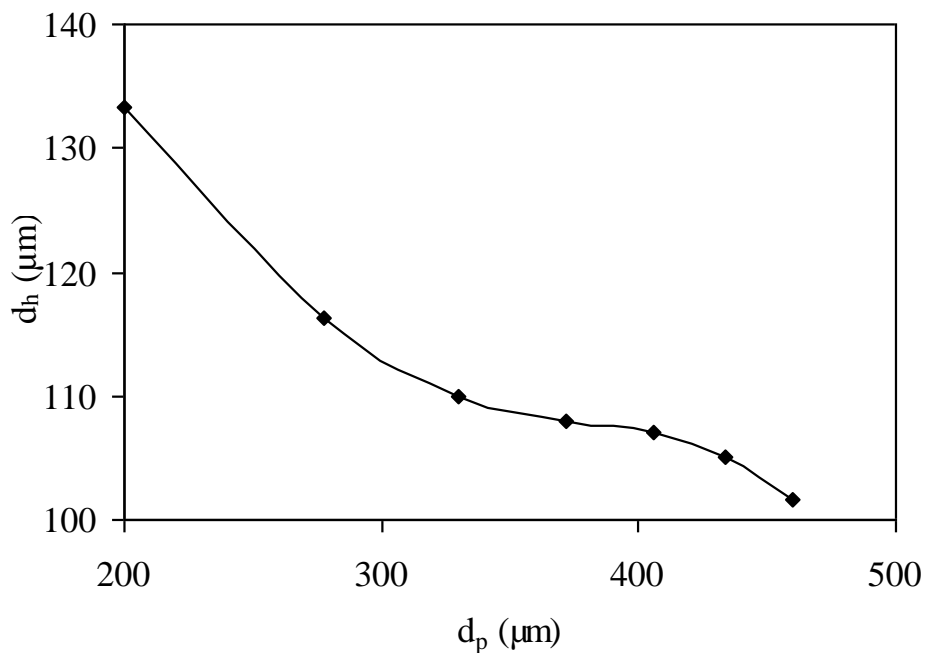


**Figure 5.** The influence of particle diameter on hydraulic diameter.

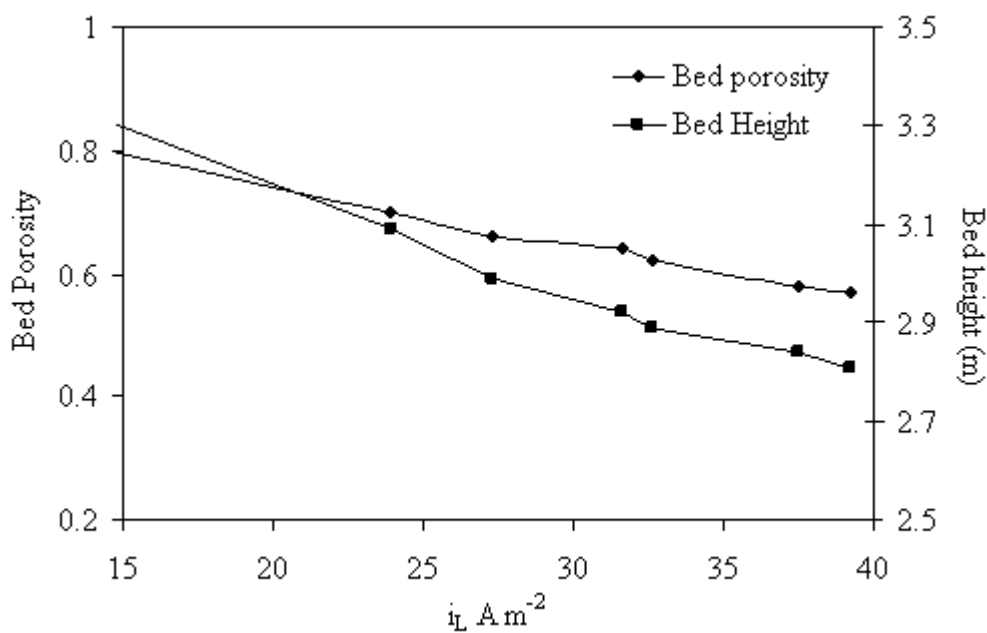


**Figure 6.** The effect of limiting current density on the bed porosity and bed expansion.

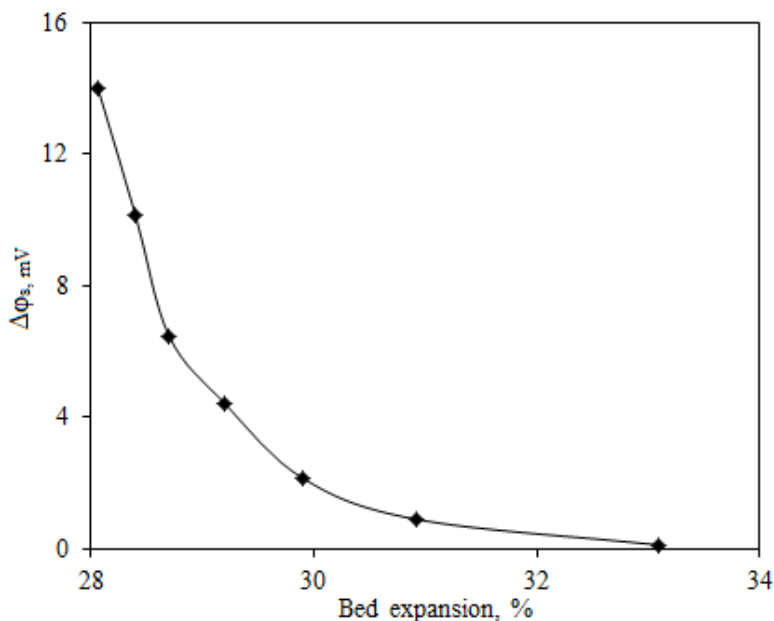


**Figure 7.** Variation of potential with bed expansion

The bed expansions greatly affect the effective conductivity of the electrolyte. The electrolyte conductivity decreased with bed expansions due to an increase in the particle-particle distance with bed expansion and the charge-transfer rate in the solid phase dominates current flows in expanded bed electrodes. The electrolyte conductivity decreased with bed expansion and in turn reduces the potential of the electrolyte [Figure 7].

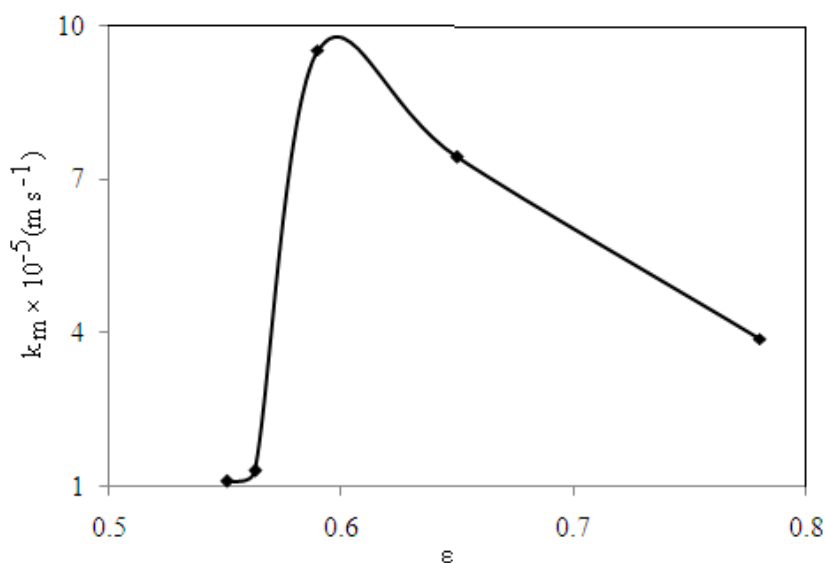


**Figure 8.** Effect of bed porosity on mass transfer coefficient.

The effective movement of the particles at optimum bed porosity condition would yield maximum transfer coefficients. The present simulated data on electrolyte-wall mass transfer coefficient is plotted against bed porosity  $\varepsilon$  [Figure 8]. It can be ascertained from the figure that the mass transfer coefficient decreases as the bed porosity increases and reached a maximum value at  $\varepsilon = 0.6$ . Further increase in the bed porosity decreases mass transfer coefficient. This is an interesting observation which can be explained that the hydrodynamic behavior of expanded bed plays an important role on mass transfer coefficient. At low porosity, i.e., around 0.5 of  $\varepsilon$ , the bed operates under turbulent fluidization where the particles forms clusters at the bottom and disperses at the top where particle individual suspension is very much limited. An increase in the bed porosity decreases the cluster formation and enhances the individual particle suspension resulting in a decreased mass transfer coefficient. On the other hand at high porosity i.e., around 0.6 and above, the bed behaves under pneumatic conveying where the particles are evenly suspended throughout the bed and an increase in the bed porosity beyond 0.6 decreases mass transfer coefficient.

The present model simulation on effect of particle size for bed porosity has been compared with the experimental data reported due to Carbin and Gabe in Figure 9. It can be ascertained that the present model simulations match satisfactorily with the data reported by Carbin and Gabe [12].

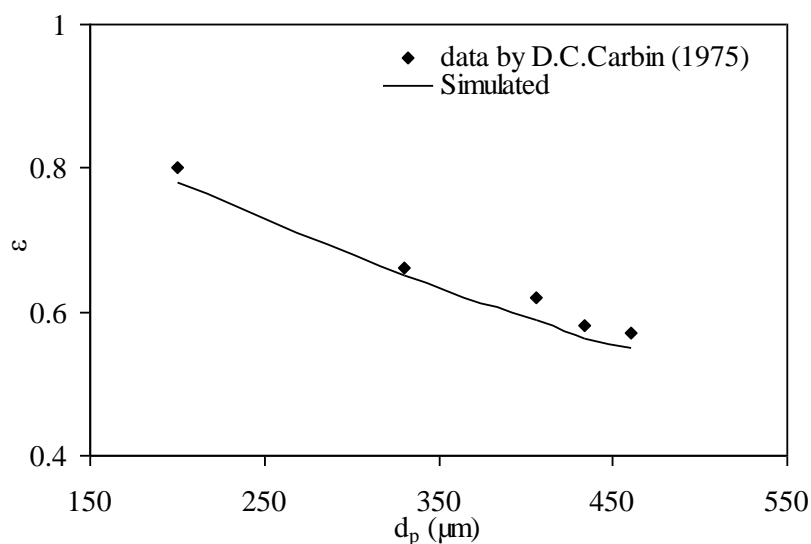


**Figure 9.** Comparison of model simulation with data due to Carbin and Gabe [12].

#### 4. CONCLUSIONS

Two-Dimensional model has been developed to predict the particle behavior in expanded bed electrode. Based on the observation, the following conclusions can be made.

1. The electrode thickness increases with increase in potential drop.
2. The mass transfer coefficient depends on the bed porosity.
3. The potential decreases with an increase bed expansion.
4. Both particle size and bed expansion influence the limiting current density.
5. The hydraulic diameter decreases with an increase in the particle size.
6. The limiting current density, potential distribution in expanded bed is significantly influenced by the hydrodynamic parameter such as bed porosity.

### Notations

$A_s$	:	Specific surface area of the electrode ( $m^2$ )
$C_{in}$	:	Initial concentration of the effluent ( $mol\ m^{-3}$ )
$C_{out}$	:	Final concentration of the effluent ( $mol\ m^{-3}$ )
$D$	:	Diffusivity of solid particle ( $m^2s^{-1}$ )
$d_p$	:	Particle diameter ( $\mu m$ )
$d_a$	:	Mean diameter ( $\mu m$ )
$d_h$	:	Hydraulic diameter ( $\mu m$ )
$F$	:	Faraday constant (96,485 C)
$I$	:	Current (A)
$I_L$	:	Limiting Current (A)
$i_L$	:	Limiting Current density ( $Am^{-2}$ )
$K$	:	Constant
$\kappa_s$	:	Apparent electrolyte conductivity ( $S\ m^{-1}$ )
$\kappa_{s0}$	:	Pure electrolyte conductivity ( $S\ m^{-1}$ )
$k_m$	:	Mass transfer coefficient ( $m\ s^{-1}$ )
$L$	:	Bed height (m)
$n$	:	No. of electrons
$\Delta P$	:	Total pressure drop (K Pa)
$U_{mf}$	:	Minimum fluidization velocity ( $m\ s^{-1}$ )
$U_t$	:	Particle terminal velocity ( $m\ s^{-1}$ )
$U_l$	:	Electrolyte velocity ( $m\ s^{-1}$ )
$V_v$	:	Volume of voids
$V_s$	:	Total volume of solids
$Re$	:	Reynolds number
$Sc$	:	Schmidt number

### Greek symbols

$\varepsilon$	:	Bed porosity
$\nu$	:	Kinematic viscosity ( $m^2\ s^{-1}$ )
$\rho_l$	:	Electrolyte density ( $kg\ m^{-3}$ )
$\rho_s$	:	Electrode density ( $kg\ m^{-3}$ )
$\mu_l$	:	Electrolyte viscosity ( $kg\ m^{-1}s^{-1}$ )
$\phi_s$	:	Electrolyte potential (mV)

$\phi_m$  : Electrode potential (mV)

## References

1. J.R., Backhurst, F.Goodridge, J.M. Coulson, R.E. Plimley, *J. Electrochem. Soc.*, 116 (1969) 1600.
2. A.Welmers, W.P.M. Van Swaau, A.A.C.M. Beenackers, *Electrochimica Acta*, 22 (1977) 1277.
3. L. LeRoy L, *Electrochimica Acta*, 23 (1978) 815.
4. N.Bertrand, F.Maura, P. Duverneuil, *Surf. Coat. Technol.* 200 (2006) 6733.
5. E. Hadzismajlovic, K.I. Popov, M.G. Pavlovic, *Powder Tech.*, 86 (1996) 145.
6. F.Couret,, *J. App. Electrochem.*, 10 (1980) 687.
7. M. Zhoua, Z.Wu, X. Mab, Y. Cong, Q. Yea, D.Wang, *Sep.Purific.Tech.*, (2004) 81.
8. K.Sivakumar, R.Thilakavathi, N.Balasubramanian C.Ahmed Basha, *Int. J. Chem. Reactor Eng.*, 6 (2008) A 41.
9. R.Thilakavathi, N. Balasubramanian, C. Ahmed Basha *J. Hazard. Material*, 162 (2009) 154.
10. K.Scott, *Electrochemical Reaction Engineering*, Academic Press (1991).
11. F.Good Ridge, K.Scott, *Electrochemical Process Engineering*, Plenum Press,New York, 1995.
12. D.C. Carbin, D.R. Gabe, *J. of Applied Electrochem.*, 5 (1975)129.
13. J.L.Nava, M.T.Oropeza, C.Ponce de León, J. González-García, A.J. Frías-Ferrer, *Hydrometall.*, 91 (2008) 98.
14. H.Miura, T. Takahashi, J.Ichikawa, Y.Kawase, *Powder Tech.*, 117 (2001) 239.
15. N.Balasubramanian, C. Srinivasakannan, *Adv. Powder Tech.*, 1 (2005) 1..
16. D.C. Carbin, D.R. Gabe, *Electrochimica Acta* , 19 (1974 ) 645.